molecular pharmaceutics

pubs.acs.org/molecularpharmaceutics

Article

Opalescence Arising from Network Assembly in Antibody Solution

Yoshitaka Nakauchi, Suguru Nishinami, Yusuke Murakami, Toshihiko Ogura, Hideaki Kano, and Kentaro Shiraki*

Cite This: *Mol. Pharmaceutics* 2022, 19, 1160−1167

Read Online

ACCESS | Metrics & More | Article Recommendations

ABSTRACT: Opalescence of therapeutic antibody solutions is one of the concerns in drug formulation. However, the mechanistic insights into the opalescence of antibody solutions remain unclear. Here, we investigated the assembly states of antibody molecules as a function of antibody concentration. The solutions of bovine gamma globulin and human immunoglobulin G at around 100 mg/mL showed the formation of submicron-scale network assemblies. The network assembly resulted in the appearance of opalescence with a transparent blue color without the precipitates of antibodies. Furthermore, the addition of trehalose and arginine, previously known to act as protein stabilizers and protein aggregation suppressors, was able to suppress the opalescence arising from the network assembly. These results will provide an important information for evaluating and improving protein formulations.

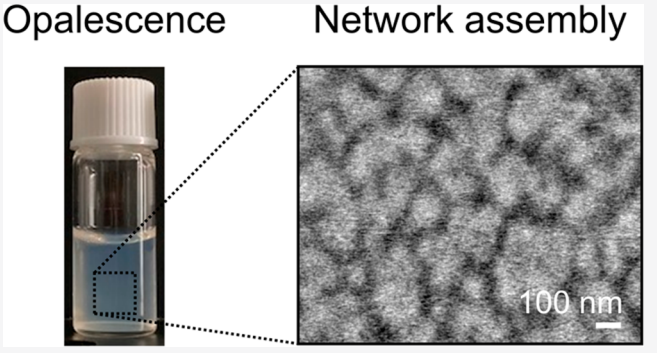

KEYWORDS: *opalescence, network assembly, liquid−liquid phase separation, antibody, additive*

INTRODUCTION

The property of opalescence has also been reported in proteins, where it refers to the cloudiness or turbidity of the protein solution.[1] In general, opalescence occurs via two optical mechanisms, namely Rayleigh scattering and Mie scattering.[2] Rayleigh scattering is the elastic scattering of light by small particles, such as protein monomers and oligomers, having a diameter much smaller than the wavelength of incident light. In contrast, Mie scattering refers to the elastic scattering of light by large particles, like protein amorphous aggregates, with a diameter similar to or larger than the wavelength of the incident light. According to European Pharmacopoeia, opalescence is quantified in terms of a nephelometric turbidity unit, which denotes the amount of scattered light detected at a scattering angle of 90°.[3]

Therapeutic antibody formulations often display an opalescence appearance, despite their great target specificity and efficiency.[1,4] Clinically, subcutaneous (SC) route is preferred for the administration of biologics owing to low cost, ease of application, and lower risk of complications. However, SC administration imposes a limitation of volume and the dosage is several mg kg^{-1}, requiring the antibodies to be concentrated,[5,6] which strongly promotes opalescence and viscosity of antibody formulations.[7,8] Recently, the development of syringe and the improvement of formulation form have been done to overcome these challenges to facilitate the delivery of large amounts of drug via SC route.[9] The opalescence of antibody formulations is considered to possibly lead to the loss of structural stability and biological function. Besides this, it hinders the development of a placebo formulation for clinical studies.[1,10] Several studies have reported that antibody concentration and solution conditions, including solution pH, ionic strength, and temperature, significantly affect the opalescence of antibody formulations.[11,12] The molecular mechanism responsible for this opalescence is mainly associated with the ability of antibodies to form reversible liquid droplets via liquid−liquid phase separation (LLPS). This characteristic of antibodies is contributed to their large and flexible structure and the presence of noncovalent protein−protein interactions, including electrostatic[4,13,14] and dipole interactions.[15,16] Various studies have reported the existence of oligomers[17,18] and the precursors of droplets and oligomers[12,19−21] in antibody solution. However, the mechanism responsible for the opalescence of antibody solutions without precipitation remains to be established.

Additives are utilized as an effective strategy to control and understand the interactions in protein solutions. Various types

Received: December 3, 2021
Revised: February 16, 2022
Accepted: March 1, 2022
Published: March 11, 2022

https://doi.org/10.1021/acs.molpharmaceut.1c00929
Mol. Pharmaceutics 2022, 19, 1160−1167

of small additives, particularly sugars,[22,23] osmolytes,[24,25] and kosmotropic salts,[26,27] have been reported to enhance the stability and solubility of proteins. Besides this, additives, like urea,[28] guanidine hydrochloride,[29] and chaotropic salts,[30] are known to suppress protein aggregation. Among these, arginine hydrochloride (ArgHCl) is the most versatile additive that has been widely used in protein solution for suppressing protein aggregation,[31,32] enzyme inactivation,[33] and nonspecific surface adsorption.[34,35] In particular, ArgHCl is known to improve the viscosity,[36] opalescence,[37] and LLPS[38,39] of highly concentrated antibody solutions. Recently, allantoin, hydantoin, and caffeine, having a different chemical backbone from arginine, have also been proposed as possible substitutes of ArgHCl for certain applications.[40−43]

Here, we reported the nanoscale network assembly of antibodies at high concentrations with the aim to propose a unified mechanism for the opalescence of antibody formulation depending on the antibody concentrations. We investigated two polyclonal antibodies, bovine gamma globulin (BGG) and human immunoglobulin G (HGG), which also contain a large number of antibody molecules with different subclasses, specificity, and different biophysical properties, typically isoelectric points. Spectroscopic techniques, namely coherent anti-Stokes Raman scattering (CARS) and scanning electron-assisted dielectric microscopy (SE-ADM), were utilized to investigate the labile structure of antibody solutions at high concentrations. Further, we investigated the effects of trehalose and ArgHCl on the opalescence of antibody solution to elucidate their utility as additives and establish the underlying mechanisms.

EXPERIMENTAL SECTION

Materials. BGG (lot number: SLBZ2175; Sigma-Aldrich Co., St. Louis, MO, USA) at 99% purity and HGG (lot number: 180820-0256; Equitech-Bio, Inc., Kerrville, TX, USA) at 97% purity were obtained. 3-(*N*-morpholino)-propanesulfonic acid (MOPS), sodium dihydrogen phosphate, sodium chloride (NaCl), L-arginine hydrochloride (ArgHCl), fluorescein-4-isothiocyanate (FITC), and trehalose dihydrate were obtained from Wako Pure Chemical Industries, Ltd. (Osaka, Japan). All the chemicals were of reagent grade.

Preparation of Antibody Stock Solutions. The lyophilized powders of proteins BGG and HGG were dissolved in pure water to prepare antibody stock solutions (>230 mg/mL). Then, these proteins were dialyzed against pure water or buffer solutions overnight at 4 °C to remove the small impurities. The concentration of the antibodies was measured at an absorbance of 280 nm against the appropriate blank using an ultraviolet−visible spectrometer (ND-1000; NanoDrop Technologies, Inc., Wilmington, DE, USA). The extinction coefficients ($E^{1\%}_{280nm}$) of BGG and HGG were 13.8 and 13.7, respectively.[44]

Turbidity Measurement. To evaluate the opalescence appearance of the protein solutions, two turbidity measurements were conducted as follows. Each sample solution was irradiated with laser light, and the transmitted light at 550 nm was detected at an angle of 180° using an ultraviolet−visible spectrophotometer (V630; Japan Spectroscopic Co., Ltd., Tokyo, Japan), while the scattered light at 510 nm was detected at a scattering angle of 90° using a spectrofluorometer (FP-6500; Japan Spectroscopic Co., Ltd., Tokyo, Japan). The sample solutions containing 0−230 mg/mL antibody and 0−1000 mM additives were transferred to a quartz cell with a 1 mm path length, and measurements were performed at 25 °C.

Microscopic Imaging. The morphology of the microscale assemblies of antibodies was observed using bright-field or fluorescence microscopy. To prepare stained BGG samples, the primary amine groups of lysine residues present on the surface of BGG were chemically modified using FITC. BGG solutions at 9−230 mg/mL concentrations were prepared by mixing FITC-labeled BGG with unlabeled BGG in 10 mM MOPS buffer (pH 7.0) at a ratio of less than 1% labeled BGG. The samples were transferred to a 96-well microplate (product number: 3474, Corning Inc., NY, USA) and observed using a phase contrast inverted fluorescence microscope (BZ-X710, Keyence Inc., Osaka, Japan). The FITC-labeled BGG molecules were detected using excitation and emission maxima of 470 and 525 nm, respectively. Notably, no significant differences were observed between the bright-field microscopic images of FITC-labeled and unlabeled BGG molecules.

CARS Imaging. Label-free antibodies forming microscale assemblies were observed using a multiplex CARS spectroscopic imaging system.[45] The main laser source was a custom-made, dual-fiber output synchronized laser source (OPERA HP, Leukos, Limoges, France). In the laser housing, the master laser output, with a wavelength of 1064 nm, temporal duration of 50 ps, and repetition rate of 1 MHz, was divided into two. One output was introduced into the large-mode area photonic crystal fiber and used as the pump beam, ω_1, which was collimated by a collimator lens (F810APC-1064, Thorlabs, Newton, NJ, USA). The other output was injected into a photonic crystal fiber to obtain ultra-broad-band supercontinuum radiation ranging from visible to near-infrared (NIR). The NIR spectral components of the SC were selected using an optical filter (IR80, Kenko-optics, Tokyo, Japan) and were used as the Stokes beam (ω_2). The SC was collimated by an off-axis parabolic mirror (RC04APC-P01, Thorlabs) to avoid chromatic dispersion. The two beams were superimposed by a notch filter (NF03-532/1064E-25, Semrock, Rochester, NY, USA) and guided into a modified inverted microscope (ECLIPSE Ti with modification, Nikon, Tokyo, Japan) in collinear geometry. Two laser pulses were tightly focused on the sample through a microscope objective (CFI Plan Apo 60× NA 1.27, water-immersion, Nikon). The samples were placed on a piezoelectric stage (Nano-LP200, Mad City Labs, Madison, WI, USA) for three-dimensional (*x*, *y*, and *z*) position selection. The full scanning range of the *xyz*-piezo stage was 200 × 200 × 200 μm^3. The second-harmonic generation (SHG), third-harmonic generation (THG), and ultra-multiplex CARS signals were collected using a second objective lens (Plan S Fluor 40× NA 0.6, Nikon) and spectrally separated by a dichroic mirror. The CARS signal transmitted through the dichroic mirror was detected using a spectrometer (LS785, Princeton Instruments, Trenton, NJ, USA) equipped with a CCD camera (BLAZE 100HR, Princeton Instruments). The spectral coverage and spectral resolution of the CARS signal were ∼3500 and 8 cm^{-1}, respectively. The SHG and THG signals reflected by the dichroic mirror were detected using a spectrometer (SpectraPro300i, Princeton Instruments) equipped with a CCD camera (PIXIS 100 B, Princeton Instruments). The exposure time at each spatial position was 50 ms for signal detection. The image size in pixels and microns were 101 × 101 pixels and 50 × 50 μm^2, respectively, and the step size was 0.5 μm.

https://doi.org/10.1021/acs.molpharmaceut.1c00929
Mol. Pharmaceutics 2022, 19, 1160−1167

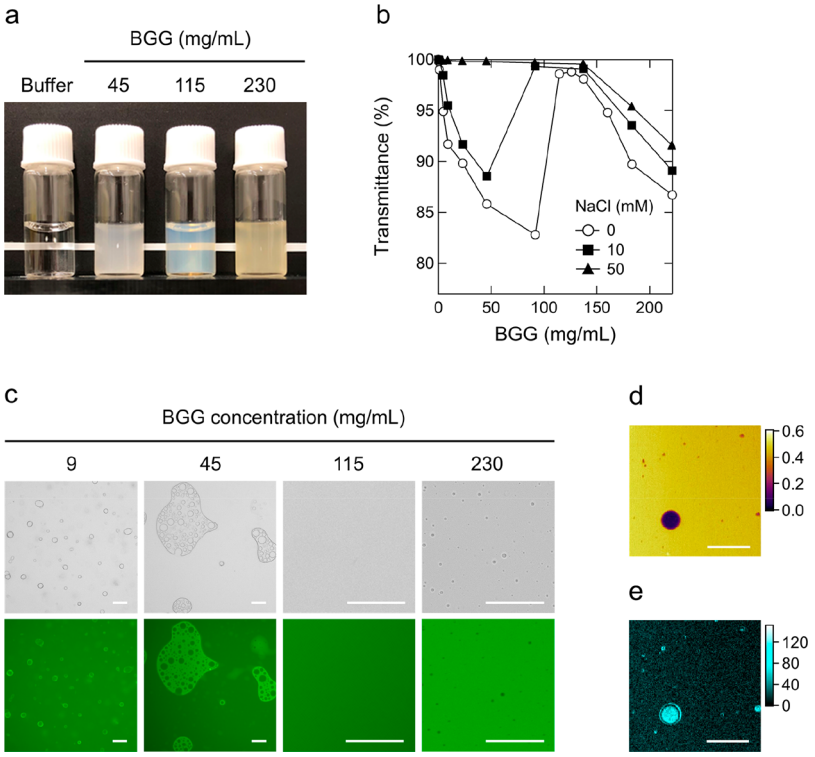

Figure 1. Opalescence arising from the microscale assembly of antibodies. (a) Visual appearance of BGG solutions at different concentrations. The white horizontal line is a white paper placed on the other side of the test tubes. (b) Quantitative measurement of light transmittance for 0−230 mg/mL BGG solutions in the absence or presence of NaCl. The values were obtained in a single experiment. (c) Bright-field (upper) and fluorescence (lower) micrographs for FITC-labeled BGG solutions. (d) CARS at 2939 $cm^{-1}$and (e) THG images for unlabeled BGG solution at 230 mg/mL. All the samples were prepared in 10 mM MOPS buffer (pH 7.0). Scale bars represent 50 μm.

SE-ADM Imaging. A structure consisting of nanoscale networks of antibodies in solutions was observed using a high-resolution SE-ADM imaging system.[46−48] This system involved a thermal field emission scanning electron microscope (SU5000, Hitachi High-Tech Co., Japan) at room temperature. A 1.0 μL aliquot of a sample solution containing 9−230 mg/mL fluorescently stained BGG and 10 mM MOPS buffer (pH 7.0) was transferred to a sample holder mounted onto the SEM stage. The detector terminal was connected to a preamplifier under the holder.[46] The electrical signal from the preamplifier was fed into an analog-to-digital converter after low-pass filtering, as previously described.[47,48] The SE-ADM images of 1280 × 1020 pixels were captured at a magnification of 20,000−50,000 at a scanning time of 40 s, working distance of 7 mm, electron beam acceleration voltage of 3.5 kV, and current of 10 pA.

The SE-ADM signals from SU5000 were transferred to a personal computer (Intel Core i7, 3.8 GHz, Windows 10). The high-resolution SE-ADM images from the low-pass filter and the scanning signals were then processed using MATLAB R2020a software with an image-processing toolbox (Math Works Inc., Natick, MA).[46−48] The SE-ADM images were filtered using a two-dimensional (2D) Gaussian filter (GF) with a kernel size of 7 × 7 pixels and a radius of 1.2σ, where σ is the half-width of the Gaussian function. Background subtraction was performed by subtracting the SE-ADM images from the filtered images using a broad GF (400 × 400 pixels, 200σ).

RESULTS

Opalescence of Antibody Solutions Depending on the Concentration. The opalescence behavior of BGG solutions was investigated at room temperature and physiological pH. The gamma globulin is a mixture of total IgGs in sera, and most of their isoelectric points are in the pH range of 7−9, with some having acidic pI. In a previous study, it has been suggested that antibody solutions show opalescence well at pH near the pI of proteins.[12] Microscopic images for the visual appearance of BGG solutions at different concentrations are shown in Figure 1a. The test tube filled with buffer is clearly visible in these images. An increase in BGG concentration induced changes in the visual appearance of BGG solutions. BGG solutions prepared at 46 and 230 mg/mL concentrations without NaCl appeared cloudy. In comparison to this, BGG solution at 115 mg/mL concentration was also slightly turbid in comparison to buffer solution; however, the sample solution was clear in this case. The overnight incubation of the opalescent solutions of BGG at 46, 115, and 230 mg/mL at room temperature resulted in the precipitation of only the 46 mg/mL solution. Following this, nonprecipitating opalescent solutions of 115 and 230 mg/mL concentrations were centrifuged at 18,800g for 20 min, and a liquid−liquid phase separation (LLPS) was observed only for 230 mg/mL solution, with more protein-rich phase (lower phase) than protein-poor phase (upper phase). As shown in Figure 1b, the quantity of transmitted light decreased with an increase in the concentration of BGG from 0 to 100 mg/mL without NaCl. In contrast, the transmittance of light increased at BGG concentrations of 115−145 mg/mL. Addition of NaCl suppressed the turbidities of BGG solutions.

https://doi.org/10.1021/acs.molpharmaceut.1c00929
Mol. Pharmaceutics 2022, 19, 1160−1167

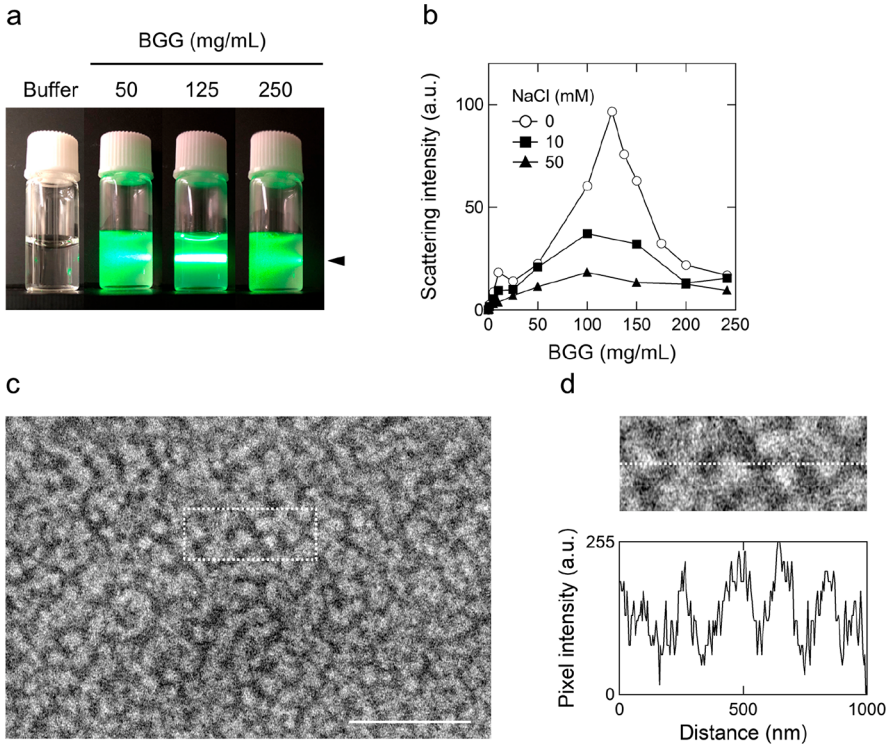

Figure 2. Opalescence arising from the nanoscale network assembly of antibodies. (a) Visual appearance of BGG solutions at different concentrations. Each sample was irradiated with laser light at 532 nm from a certain position (indicated by black triangle arrow). (b) Quantitative measurement of the light scattering intensity for 0−230 mg/mL BGG solutions, in the absence or presence of NaCl, monitored at a scattering of 90°and wavelength at 510 nm. The values were obtained in a single experiment. (c) SE-ADM image for 115 mg/mL BGG solutions. The black area shows the presence of BGG, and the pixel intensity corresponds to 0. Scale bar represents 1 μm. (d) Mesh size of the network assembly observed in 115 mg/mL BGG solution. The SE-ADM image is an expansion of the area surrounded by the white dotted line shown in (c). Pixel intensity shows the density of BGG molecules present on the white dotted line in the enlarged image. All the samples were prepared in 10 mM MOPS buffer (pH 7.0).

To identify the reason for the cloudy appearance of BGG solutions, we investigated the formation of microscale assemblies with increasing BGG concentrations. Figure 1c shows the bright-field and fluorescence images of BGG solutions containing FITC-labeled BGG. BGG solutions at 9 and 46 mg/mL showed the presence of droplet-like assembly that was found to be spherical at the BGG concentration of 9 mg/mL, whereas the droplets at 46 mg/mL concentration were spherical and multiphased. In the case of 115 mg/mL BGG solution, no microscale assemblies were observed, while the BGG solution at 230 mg/mL BGG concentration showed the presence of protein-poor droplets. A multiplex CARS microscope was also used to observe the BGG droplets, and label-free images were acquired for the assembly of biomolecules. Figure 1d shows the CARS images for unlabeled BGG solution at 230 mg/mL. In the CARS image, the peak intensities for BGG (at 2939 cm^{-1} for CH_3 symmetric stretching vibration) derived outside the droplets were found to be much larger than the intensities recorded inside. It should be noted that the inside of the droplet has a noticeable CH_2 stretching vibration (at 2850 cm^{-1}) compared to the outside. Perhaps, BGG solution contains aliphatic molecules that cannot be removed by dialysis. In general, the THG process gives a signal when there is a difference in the refractive index. Thus, the boundary, interface, and assemblies with submicrometer scale should be THG-active. As shown in Figure 1e, THG activity was observed in the case of protein-poor BGG droplets. In contrast, the SHG process that gives signals in the case of noncentrosymmetric structures was not observed in the present study, indicating the absence of noncentrosymmetric structures such as the amyloid[49] or crystal-like ordered structures in the BGG solutions (data not shown).

Nanoscale Network Assembly of Highly Concentrated Antibodies. We further investigated the submicron-scale assembly states of the antibody solutions using SE-ADM. Figure 2a shows the irradiation of 4 and 230 mg/mL BGG solutions with green laser, resulting in the spreading of light throughout the solution. Interestingly, a strong light scattering was observed only in the path of laser beam in the case of 115 mg/mL BGG solution. Figure 2b shows the quantitative values for scattered light intensity in BGG solutions recorded at a scattering angle of 90°. Addition of 10 and 50 mM NaCl suppressed the scattering of light, indicating that electrostatic interaction was responsible for the opalescence. Next, SE-ADM was used to investigate the mechanism responsible for opalescence in antibody solutions without microscale assemblies. SE-ADM allows the direct observation of nanoscale objects in solution, subjecting samples to very little stress. Figure 2c shows the SE-ADM images for the nanoscale network assembly of BGG at 115 mg/mL, characterized by the presence of almost equal volumes of the diluted and condensed phases of BGG molecules. The network assembly showed mesh size of hundreds of nanometers, while the width of BGG condensates comprising the network structure was found to be tens of nanometers (Figure 2d).

https://doi.org/10.1021/acs.molpharmaceut.1c00929
Mol. Pharmaceutics 2022, 19, 1160−1167

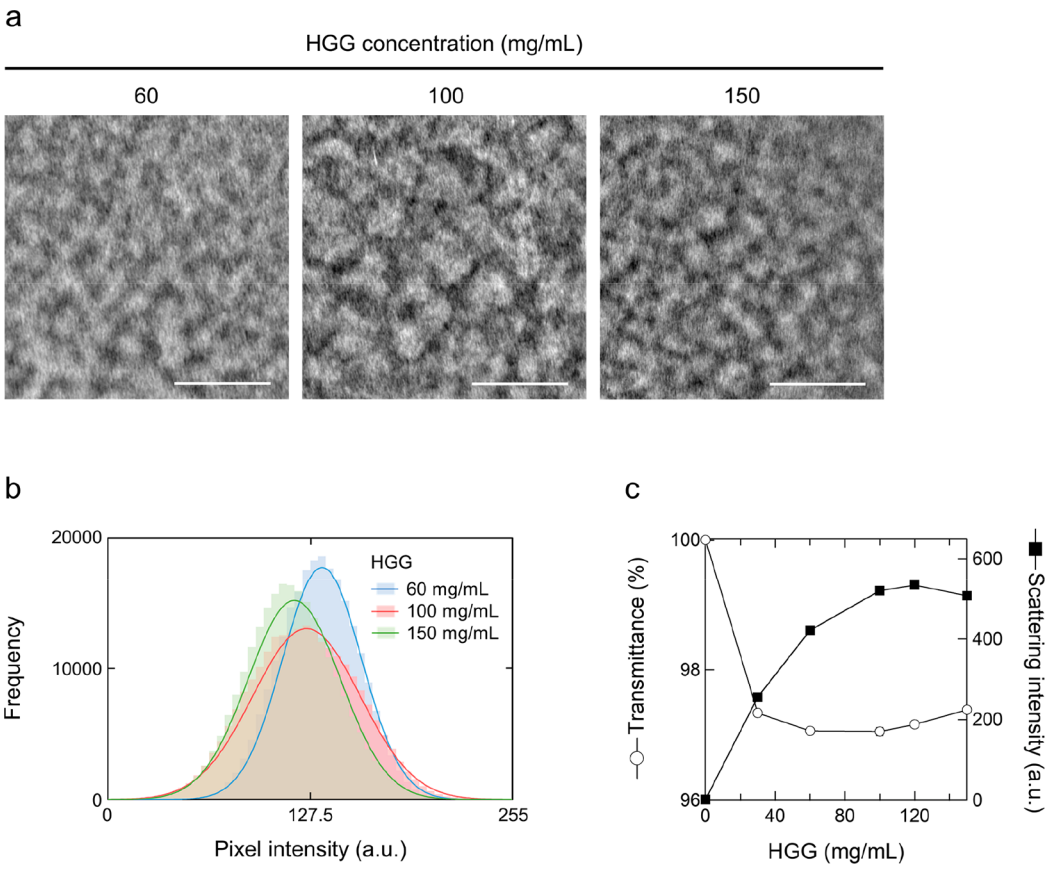

Figure 3. Size and density of network assembly depending on antibody concentrations. (a) SE-ADM images of HGG solutions at different concentrations. The black area shows the presence of BGG, and the pixel intensity corresponds to 0. Scale bars represent 500 nm. (b) Histograms for the two-dimensional pixel intensity of SE-ADM images shown in (a). Solid lines represent the Gaussian distribution curves calculated for each histogram. (c) Quantitative measurement of light transmittance and scattered light intensity for 0−150 mg/mL HGG solutions as a function of antibody concentrations. The determined values were the averages of triplicate experiments. All the samples were prepared in 20 mM Na phosphate buffer (pH 7.0).

The formation of nanoscale network assembly was also investigated in HGG solutions. Unlike BGG solutions, HGG did not exhibit any precipitation or LLPS in water even when subjected to centrifugation at 18,800*g* for 20 min. Figure 3a shows the SE-ADM images for HGG solutions at 60−150 mg/mL. As expected, HGG solutions showed the formation of network assemblies in a concentration-dependent manner. Similar to BGG, the mesh size of the HGG network assembly was also measured to be around hundreds of nanometers, and it changed as a function of HGG concentration. The mesh size at 60 and 100 mg/mL appeared to be larger than 150 mg/mL, consistent with the light scattering intensity. The statistical analysis for the mesh size of network assemblies is shown in Figure 3b. The histogram analysis of the two-dimensional pixel intensity for each SE-ADM image showed that the density of antibodies in network assemblies increased as a function of antibody concentration. The maximum distribution of antibodies in the concentrated and diluted phases was attained at 100 mg/mL concentration. As shown in Figure 3c, the opalescence in HGG solutions was found to be concentration-dependent. The light transmittance decreased until 100 mg/mL HGG concentration; however, it increased with further increase in HGG concentrations. These results indicated that the network assemblies were formed at high concentrations of HGG solution, in the range of 60 and 150 mg/mL, even in the presence of slight differences in the mesh size.

Ultracentrifugation of the Network Assembly. Next, the change in the opalescence of antibody solutions arising due to the application of mechanical stress on the network assembly was studied using ultracentrifugation. Figure 4

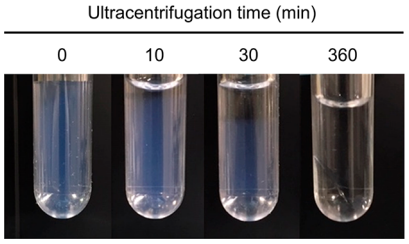

Figure 4. Ultracentrifugation of antibody solution displaying the network assembly.

shows the visual appearance of the HGG solutions containing the network assembly before and after ultracentrifugation. Before ultracentrifugation, the HGG solution was characterized by an opalescent appearance with a transparent blue color. Further, the ultracentrifugation of HGG solution at 120,000 rpm resulted in the formation of clean/opalescent phase separation in a nonequilibrium manner. Ultracentrifugation of the solution for a sufficiently long time (360 min) divided the opalescent solution into two clear phases with an interface. The supernatant after ultracentrifugation for 360 min did not

https://doi.org/10.1021/acs.molpharmaceut.1c00929
Mol. Pharmaceutics 2022, 19, 1160−1167

contain any protein. This might be attributed to the removal of water molecules present in the network assembly by ultracentrifugation. In particular, ultracentrifugation of protein solutions for several hours results in the formation of glass-like protein condensates.[50]

100 mg/mL of HGG solution with 50 mM MOPS buffer (pH 7.0) was ultracentrifuged at 120,000 rpm and 25 °C for the indicated time periods.

Effects of Additives on the Opalescence Arising from the Network Assembly. Development of stable and biologically active biopharmaceuticals demands the prevention of opalescence of antibody solutions. Trehalose is widely utilized as a protein stabilizer, while ArgHCl has been employed to suppress protein aggregation. The present study investigated the effects of trehalose and ArgHCl on the opalescence arising from the network assembly. Figure 5a shows the SE-ADM images for the 80 mg/mL HGG solution in the presence of trehalose and ArgHCl. In the absence of additives, the network assemblies were observed in HGG solution at concentrations ~80 mg/mL (Figure 3a). However, the HGG network assembly was found to be broken and dissolved in the presence of 300 mM ArgHCl. Further, the addition of 300 mM trehalose suppressed the formation of network structural assembly and resulted in the formation of non-networked oligomers. These additives displayed a concentration-dependent suppression of opalescence in the order, ArgHCl > NaCl > trehalose (Figure 5b). These results suggested that trehalose and ArgHCl induced independent effects on the opalescence arising from the network assembly. This might be attributed to the preferential interaction of trehalose,[51,52] whereas cation−pi, pi−pi, and electrostatic interactions might be involved in the interaction of ArgHCl with antibody molecules.[53−55] The study also evaluated the combined effects of these additives on the opalescence of antibody solutions. Figure 5c shows the scattered light intensity for 80 mg/mL HGG solutions in the presence of 300 mM trehalose and ArgHCl. The mixture of trehalose and ArgHCl was found to be slightly more effective in suppressing opalescence as compared to the use of individual additives.

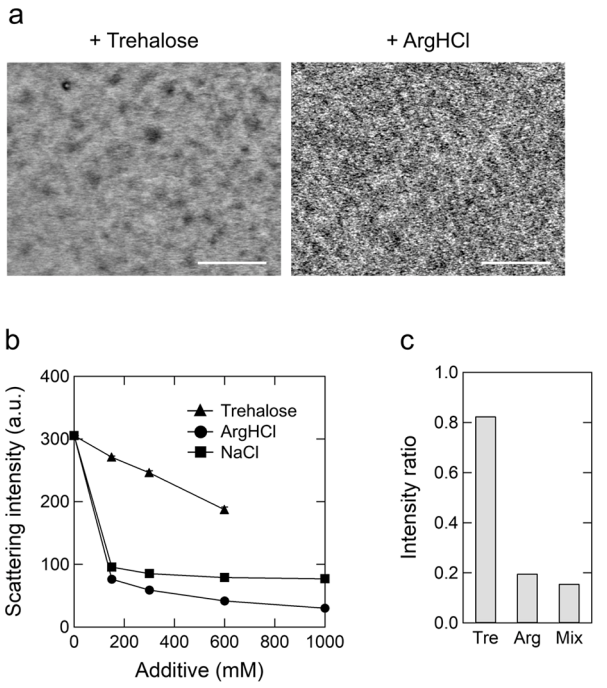

Figure 5. Effects of additives on opalescence arising from the network assembly. (a) SE-ADM images for 80 mg/mL HGG solution, in the presence of 300 mM trehalose or ArgHCl. Scale bars indicate 500 nm. (b) Quantitative measurement of light scattering intensity for 80 mg/mL HGG solution in the presence or absence of additives (i.e., trehalose, ArgHCl, or NaCl). (c) Ratio of intensity for 80 mg/mL HGG solution with 300 mM trehalose and ArgHCl; the intensity of HGG solution without additives corresponds to 1. The determined values were the averages of triplicate experiments. All the samples were prepared in 10 mM MOPS buffer (pH 7.0).

DISCUSSION

This paper investigated the size and morphology of antibody solutions at high concentrations using fluorescence microscopy, CARS, and SE-ADM. The results showed that there was a relationship between the opalescence appearance and the formation of nanoscale network assembly or oligomer of antibodies. The formation mechanism of nanoscale network assemblies is considered as follows. In BGG solutions, the network assembly was observed at the concentrations lying between two critical concentrations, which were related to the antibody solubility (Figure 1c). For HGG solutions, the opalescence without precipitation was observed at higher HGG concentrations, which was similar to the opalescence observed for BGG solution containing small amounts of NaCl. The opalescence without precipitation has been previously reported in the case of therapeutic monoclonal antibody formulations, where LLPS was induced particularly at low temperature and low ionic strength, or in the presence of molecular crowders such as polyethylene glycol.[12,19,38] The formation of a polymer-rich phase in the metastable region of LLPS, existing between binodal and spinodal curves, involves the initiation of nucleation as a local phenomenon. In the unstable region that arises due to spinodal decomposition, small fluctuations in the polymer density are observed in the long-range order. These fluctuations further result in the formation of areas without sharp interface instead of droplets, which probably represents the network assembly of antibodies. Notably, the size of the network assembly of antibodies was in the range of tens to hundreds of nanometers. This might be driven by the charge distribution and dipole moment on the surface of the antibodies, involving Fab−Fab and Fab−Fc interactions.[56−60] The formation of a network probably requires charge asymmetry and local interactions.

Trehalose and ArgHCl successfully suppressed the opalescence of antibody solutions. In the presence of trehalose, the network structure of antibodies appeared to favor more compact structures such as monomers and oligomers. Trehalose is a protein stabilizer that increases the surface tension of water, away from the protein−water interface, and enhances protein hydration.[51,52] On the other hand, the suppression effect of ArgHCl on the opalescence was higher than that of NaCl and trehalose. ArgHCl interacts directly with the surface of proteins via cation−pi and pi−pi interactions mediated by the guanidinium group of the side chain and electrostatic interactions between its charged backbone and the guanidinium group.[53−55] Thus, the effects of trehalose and ArgHCl on opalescence were mutually independent, further supporting the enhanced combinatorial effect of ArgHCl and trehalose observed in the present study.

https://doi.org/10.1021/acs.molpharmaceut.1c00929
Mol. Pharmaceutics 2022, 19, 1160−1167

CONCLUSIONS

This paper identified the submicron network-like phase separation of antibodies, which suggests a mechanistic insight into the opalescence of antibody solution as a function of its concentration. Arginine and trehalose successfully suppressed the opalescence of the antibody solutions by affecting the network assembly. These results will provide a fundamental information for the development of liquid biopharmaceuticals and for understanding the protein nature.

AUTHOR INFORMATION

Corresponding Author

Kentaro Shiraki − *Faculty of Pure and Applied Sciences, University of Tsukuba, Tsukuba 305-8573, Japan;* orcid.org/0000-0003-3438-4076; Email: shiraki@bk.tsukuba.ac.jp

Authors

Yoshitaka Nakauchi − *Faculty of Pure and Applied Sciences, University of Tsukuba, Tsukuba 305-8573, Japan*

Suguru Nishinami − *Faculty of Pure and Applied Sciences, University of Tsukuba, Tsukuba 305-8573, Japan*

Yusuke Murakami − *Ph.D. Program in Humanics, University of Tsukuba, Tsukuba 305-8577, Japan; International Institute for Integrative Sleep Medicine (WPI-IIIS), University of Tsukuba, Tsukuba 305-8575, Japan*

Toshihiko Ogura − *Health and Medical Research Institute, National Institute of Advanced Industrial Science and Technology (AIST), Tsukuba 305-8566, Japan;* orcid.org/0000-0001-8953-6562

Hideaki Kano − *Department of Chemistry, Kyusyu University, Fukuoka-shi 819-0395, Japan*

Complete contact information is available at: https://pubs.acs.org/10.1021/acs.molpharmaceut.1c00929

Funding

This work was partly supported by JSPS KAKENHI (grant number 18H02383).

Notes

The authors declare no competing financial interest.

ACKNOWLEDGMENTS

We are grateful to Dr. Atsushi Hirano (AIST, Japan) and Dr. Shunsuke Tomita (AIST, Japan) for valuable discussion and introducing us as collaborators.

ABBREVIATIONS

ArgHCl, arginine hydrochloride; HGG, human immunoglobulin G; BGG, bovine gamma globulin; SE-ADM, scanning electron-assisted dielectric microscopy; CARS, coherent anti-Stokes Raman scattering; LLPS, liquid−liquid phase separation; GLPC, glass-like protein condensates

REFERENCES

(1) Raut, A. S.; Kalonia, D. S. Pharmaceutical perspective on opalescence and liquid−liquid phase separation in protein solutions. *Mol. Pharm.* **2016**, *13*, 1431−1444.

(2) Oster, G. The scattering of light and its applications to chemistry. *Chem. Rev.* **1948**, *43*, 319−365.

(3) Council of Europe 2.2.1. Clarity and degree of opalescence of liquids. In *European Pharmacopoeia*; 5th ed.; Council of Europe 2004, published 2005; Vol. *1*, pp 23−24.General Notices.

(4) Kingsbury, J. S.; Saini, A.; Auclair, S. M.; Fu, L.; Lantz, M. M.; Halloran, K. T.; Calero-Rubio, C.; Schwenger, W.; Airiau, C. Y.; Zhang, J.; Gokarn, Y. R. A single molecular descriptor to predict solution behavior of therapeutic antibodies. *Sci. Adv.* **2020**, *6*, No. eabb0372.

(5) Shire, S. J.; Shahrokh, Z.; Liu, J. Challenges in the development of high protein concentration formulations. *J. Pharm. Sci.* **2004**, *93*, 1390−1402.

(6) Dani, B.; Platz, R.; Tzannis, S. T. High concentration formulation feasibility of human immunoglobulin G for subcutaneous administration. *J. Pharm. Sci.* **2007**, *96*, 1504−1517.

(7) Woods, J. M.; Nesta, D. Formulation effects on opalescence of a high-concentration MAb. *BioProcess Int.* **2010**, *8*, 48−59.

(8) Salinas, B. A.; Sathish, H. A.; Bishop, S. M.; Harn, N.; Carpenter, J. F.; Randolph, T. W. Understanding and modulating opalescence and viscosity in a monoclonal antibody formulation. *J. Pharm. Sci.* **2010**, *99*, 82−93.

(9) Badkar, A. V.; Gandhi, R. B.; Davis, S. P.; LaBarre, M. J. Subcutaneous delivery of high-dose/volume biologics: current status and prospect for future advancements. *Drug Des., Dev. Ther.* **2021**, *15*, 159−170.

(10) Wang, W.; Singh, S.; Zeng, D. L.; King, K.; Nema, S. Antibody structure, instability, and formulation. *J. Pharm. Sci.* **2007**, *96*, 1−26.

(11) Wang, N.; Hu, B.; Ionescu, R.; Hamm, C.; Wang, N.; Mach, H.; Kirchmeier, M. J.; Sweeney, J. Opalescence of an IgG1 monoclonal antibody formulation is mediated by ionic strength and excipients. *Biopharm Int.* **2009**, *22*, 36−47.

(12) Mason, B. D.; Zhang, L.; Remmele, R. L., Jr; Zhang, J. Opalescence of an IgG2 monoclonal antibody solution as it relates to liquid−liquid phase separation. *J. Pharm. Sci.* **2011**, *100*, 4587−4596.

(13) Liu, J.; Nguyen, M. D. H.; Andya, J. D.; Shire, S. J. Reversible self-association increases the viscosity of a concentrated monoclonal antibody in aqueous solution. *J. Pharm. Sci.* **2005**, *94*, 1928−1940.

(14) Saluja, A.; Kalonia, D. S. Nature and consequences of protein−protein interactions in high protein concentration solutions. *Int. J. Pharm.* **2008**, *358*, 1−15.

(15) Yadav, S.; Shire, S. J.; Kalonia, D. S. Factors affecting the viscosity in high concentration solutions of different monoclonal antibodies. *J. Pharm. Sci.* **2010**, *99*, 4812−4829.

(16) Singh, S. N.; Yadav, S.; Shire, S. J.; Kalonia, D. S. Dipole-dipole interaction in antibody solutions: correlation with viscosity behavior at high concentration. *Pharm. Res.* **2014**, *31*, 2549−2558.

(17) Sukumar, M.; Doyle, B. L.; Combs, J. L.; Pekar, A. H. Opalescent appearance of an IgG1 antibody at high concentrations and its relationship to noncovalent association. *Pharm. Res.* **2004**, *21*, 1087−1093.

(18) Yang, T.-C.; Langford, A. J.; Kumar, S.; Ruesch, J. C.; Wang, W. Trimerization dictates solution opalescence of a monoclonal antibody. *J. Pharm. Sci.* **2016**, *105*, 2328−2337.

(19) Nishi, H.; Miyajima, M.; Nakagami, H.; Noda, M.; Uchiyama, S.; Fukui, K. Phase separation of an IgG1 antibody solution under a low ionic strength condition. *Pharm. Res.* **2010**, *27*, 1348−1360.

(20) Raut, A. S.; Kalonia, D. S. Opalescence in monoclonal antibody solutions and its correlation with intermolecular interactions in dilute and concentrated solutions. *J. Pharm. Sci.* **2015**, *104*, 1263−1274.

(21) Kheddo, P.; Bramham, J. E.; Dearman, R. J.; Uddin, S.; van der Walle, C. F.; Golovanov, A. P. Investigating liquid−liquid phase separation of a monoclonal antibody using solution-state NMR spectroscopy: effect of Arg· Glu and Arg· HCl. *Mol. Pharm.* **2017**, *14*, 2852−2860.

(22) Arakawa, T.; Timasheff, S. N. Stabilization of protein structure by sugars. *Biochemistry* **1982**, *21*, 6536−6544.

(23) Sasahara, K.; McPhie, P.; Minton, A. P. Effect of dextran on protein stability and conformation attributed to macromolecular crowding. *J. Mol. Biol.* **2003**, *326*, 1227−1237.

(24) Arakawa, T.; Timasheff, S. N. The stabilization of proteins by osmolytes. *Biophys. J.* **1985**, *47*, 411−414.

(25) Yoshizawa, S.; Oki, S.; Arakawa, T.; Shiraki, K. Trimethylamine N-oxide (TMAO) is a counteracting solute of benzyl alcohol for

multi-dose formulation of immunoglobulin. *Int. J. Biol. Macromol.* **2018**, *107*, 984−989.
(26) Arakawa, T.; Timasheff, S. N. Mechanism of protein salting in and salting out by divalent cation salts: balance between hydration and salt binding. *Biochemistry* **1984**, *23*, 5912−5923.
(27) Endo, A.; Kurinomaru, T.; Shiraki, K. Hyperactivation of α-chymotrypsin by the Hofmeister effect. *J. Mol. Catal. B: Enzym.* **2016**, *133*, S432−S438.
(28) Prakash, V.; Loucheux, C.; Scheufele, S.; Gorbunoff, M. J.; Timasheff, S. N. Interactions of proteins with solvent components in 8 M urea. *Arch. Biochem. Biophys.* **1981**, *210*, 455−464.
(29) Noelken, M. E.; Timasheff, S. N. Preferential solvation of bovine serum albumin in aqueous guanidine hydrochloride. *J. Biol. Chem.* **1967**, *242*, 5080−5085.
(30) Kudou, M.; Shiraki, K.; Fujiwara, S.; Imanaka, T.; Takagi, M. Prevention of thermal inactivation and aggregation of lysozyme by polyamines. *Eur. J. Biochem.* **2003**, *270*, 4547−4554.
(31) Iwashita, K.; Inoue, N.; Handa, A.; Shiraki, K. Thermal aggregation of hen egg white proteins in the presence of salts. *Protein J.* **2015**, *34*, 212−219.
(32) Tsumoto, K.; Ejima, D.; Kita, Y.; Arakawa, T. Review: Why is Arginine Effective in Suppressing Aggregation? *Protein Pept. Lett.* **2005**, *12*, 613−619.
(33) Yoshizawa, S.; Arakawa, T.; Shiraki, K. Thermal aggregation of human immunoglobulin G in arginine solutions: contrasting effects of stabilizers and destabilizers. *Int. J. Biol. Macromol.* **2017**, *104*, 650−655.
(34) Matsuoka, T.; Hamada, H.; Matsumoto, K.; Shiraki, K. Indispensable structure of solution additives to prevent inactivation of lysozyme for heating and refolding. *Biotechnol. Prog.* **2009**, *25*, 1515−1524.
(35) Arakawa, T.; Philo, J. S.; Tsumoto, K.; Yumioka, R.; Ejima, D. Elution of antibodies from a Protein-A column by aqueous arginine solutions. *Protein Expr. Purif.* **2004**, *36*, 244−248.
(36) Shikiya, Y.; Tomita, S.; Arakawa, T.; Shiraki, K. Arginine inhibits adsorption of proteins on polystyrene surface. *PLoS One* **2013**, *8*, No. e70762.
(37) Inoue, N.; Takai, E.; Arakawa, T.; Shiraki, K. Specific decrease in solution viscosity of antibodies by arginine for therapeutic formulations. *Mol. Pharm.* **2014**, *11*, 1889−1896.
(38) Oki, S.; Nishinami, S.; Shiraki, K. Arginine suppresses opalescence and liquid−liquid phase separation in IgG solutions. *Int. J. Biol. Macromol.* **2018**, *118*, 1708−1712.
(39) Hu, Y.; Arora, J.; Joshi, S. B.; Esfandiary, R.; Middaugh, C. R.; Weis, D. D.; Volkin, D. B. Characterization of excipient effects on reversible self-association, backbone flexibility, and solution properties of an IgG1 monoclonal antibody at high concentrations: Part 1. *J. Pharm. Sci.* **2020**, *109*, 340−352.
(40) Nishinami, S.; Yoshizawa, S.; Arakawa, T.; Shiraki, K. Allantoin and hydantoin as new protein aggregation suppressors. *Int. J. Biol. Macromol.* **2018**, *114*, 497−503.
(41) Nishinami, S.; Kameda, T.; Arakawa, T.; Shiraki, K. Hydantoin and Its Derivatives Reduce the Viscosity of Concentrated Antibody Formulations by Inhibiting Associations via Hydrophobic Amino Acid Residues. *Ind. Eng. Chem. Res.* **2019**, *58*, 16296−16306.
(42) Nishinami, S.; Ikeda, K.; Nagao, T.; Koyama, A. H.; Arakawa, T.; Shiraki, K. Aromatic interaction of hydantoin compounds leads to virucidal activities. *Biophys. Chem.* **2021**, *275*, 106621.
(43) Zeng, Y.; Tran, T.; Wuthrich, P.; Naik, S.; Davagnino, J.; Greene, D. G.; Mahoney, R. P.; Soane, D. S. Caffeine as a viscosity reducer for highly concentrated monoclonal antibody solutions. *J. Pharm. Sci.* **2021**, *110*, 3594−3604.
(44) Rosenberg, R. D.; Colman, R. W.; Lorand, L. A new haemorrhagic disorder with defective fibrin stabilization and cryofibrinogenaemia. *Br. J. Haematol.* **1974**, *26*, 269−284.
(45) Miyazaki, S.; Leproux, P.; Couderc, V.; Hayashi, Y.; Kano, H. Multimodal nonlinear optical imaging of Caenorhabditis elegans with multiplex coherent anti-Stokes Raman scattering, third-harmonic generation, second-harmonic generation, and two-photon excitation fluorescence. *Appl. Phys. Express* **2020**, *13*, 072002.
(46) Ogura, T. Nanoscale analysis of unstained biological specimens in water without radiation damage using high-resolution frequency transmission electric-field system based on FE-SEM. *Biochem. Biophys. Res. Commun.* **2015**, *459*, 521−528.
(47) Okada, T.; Ogura, T. Nanoscale imaging of untreated mammalian cells in a medium with low radiation damage using scanning electron-assisted dielectric microscopy. *Sci. Rep.* **2016**, *6*, 29169.
(48) Okada, T.; Iwayama, T.; Murakami, S.; Torimura, M.; Ogura, T. Nanoscale observation of PM2.5 incorporated into mammalian cells using scanning electron-assisted dielectric microscope. *Sci. Rep.* **2021**, *11*, 228.
(49) Ni, M.; Zhuo, S.; Iliescu, C.; So, P. T. C.; Mehta, J. S.; Yu, H.; Hauser, C. A. E. Self-assembling amyloid-like peptides as exogenous second harmonic probes for bioimaging applications. *J. Biophot.* **2019**, *12*, No. e201900065.
(50) Nakauchi, Y.; Nishinami, S.; Shiraki, K. Glass-like protein condensate for the long-term storage of proteins. *Int. J. Biol. Macromol.* **2021**, *182*, 162−167.
(51) Xie, G.; Timasheff, S. N. The thermodynamic mechanism of protein stabilization by trehalose. *Biophys. Chem.* **1997**, *64*, 25−43.
(52) Sudrik, C.; Cloutier, T.; Pham, P.; Samra, H. S.; Trout, B. L. Preferential interactions of trehalose, L-arginine. HCl and sodium chloride with therapeutically relevant IgG1 monoclonal antibodies, *mAbs*, 2017; *9*, 1155−1168.Taylor & Francis DOI: 10.1080/19420862.2017.1358328
(53) Arakawa, T.; Ejima, D.; Tsumoto, K.; Obeyama, N.; Tanaka, Y.; Kita, Y.; Timasheff, S. N. Suppression of protein interactions by arginine: a proposed mechanism of the arginine effects. *Biophys. Chem.* **2007**, *127*, 1−8.
(54) Miyatake, T.; Yoshizawa, S.; Arakawa, T.; Shiraki, K. Charge state of arginine as an additive on heat-induced protein aggregation. *Int. J. Biol. Macromol.* **2016**, *87*, 563−569.
(55) Hong, T.; Iwashita, K.; Shiraki, K. Viscosity control of protein solution by small solutes: a review. *Curr. Protein Pept. Sci.* **2018**, *19*, 746−758.
(56) Kanai, S.; Liu, J.; Patapoff, T. W.; Shire, S. J. Reversible self-association of a concentrated monoclonal antibody solution mediated by Fab−Fab interaction that impacts solution viscosity. *J. Pharm. Sci.* **2008**, *97*, 4219−4227.
(57) Yadav, S.; Laue, T. M.; Kalonia, D. S.; Singh, S. N.; Shire, S. J. The influence of charge distribution on self-association and viscosity behavior of monoclonal antibody solutions. *Mol. Pharm.* **2012**, *9*, 791−802.
(58) Buck, P. M.; Chaudhri, A.; Kumar, S.; Singh, S. K. Highly viscous antibody solutions are a consequence of network formation caused by domain−domain electrostatic complementarities: Insights from coarse-grained simulations. *Mol. Pharm.* **2015**, *12*, 127−139.
(59) Arora, J.; Hu, Y.; Esfandiary, R.; Sathish, H. A.; Bishop, S. M.; Joshi, S. B.; Middaugh, C. R.; Volkin, D. B.; Weis, D. D. Charge-mediated Fab-Fc interactions in an IgG1 antibody induce reversible self-association, cluster formation, and elevated viscosity. *mAbs* **2016**, *8*, 1561−1574 Taylor & Francis.
(60) Kopp, M. R. G.; Villois, A.; Capasso Palmiero, U.; Arosio, P. Microfluidic diffusion analysis of the size distribution and micro-rheological properties of antibody solutions at high concentrations. *Ind. Eng. Chem. Res.* **2018**, *57*, 7112−7120.